EFDA–JET–CP(08)02/13

S. Brezinsek, A.G. Meigs, S. Jachmich, M.F. Stamp, J. Rapp, R. Felton, R.A. Pitts
V. Philipps, A. Huber, R. Pugno , G. Sergienko, A. Pospieszczyk
and JET EFDA contributors

The Impact of Divertor Detachment on Carbon Sources in JET L-Mode Discharges

The Impact of Divertor Detachment on Carbon Sources in JET L-Mode Discharges

S. Brezinsek[1], A.G. Meigs[2], S. Jachmich[3], M.F. Stamp[2], J. Rapp[1,4], R. Felton[2], R.A. Pitts[5] V. Philipps[1], A. Huber[1], R. Pugno[6], G. Sergienko[1], A. Pospieszczyk[1] and JET EFDA contributors*

JET-EFDA, Culham Science Centre, OX14 3DB, Abingdon, UK

[1]Institut für Energieforschung-Plasmaphysik, Forschungszentrum Jülich[+], Association, EURATOM-FZJ, Germany
[2]EURATOM-UKAEA Fusion Association, Culham Science Centre, OX14 3DB, Abingdon, OXON, UK
[3]LPP-ERM/KMS[+], Association EURATOM-Belgian State, Belgium
[4]FOM-Rijnhuizen[+], Association EURATOM-FOM, The Netherlands
[5]CRPP-EPFL, Association EURATOM-Confdration Suisse, CH-1015 Lausanne, Switzerland
[6]Association EURATOM-Max-Planck-Institut für Plasmaphysik, D-85748 Garching, Germany
[+]Partners in the Trilateral Euregio Cluster (TEC)
** See annex of M.L. Watkins et al, "Overview of JET Results ",*
(Proc. 21[st] IAEA Fusion Energy Conference, Chengdu, China (2006)).

Preprint of Paper to be submitted for publication in Proceedings of the
18th Plasma Surface Interactions in Controlled Fusion Devices, Toledo, Spain
(26th May 2008 - 30th May 2008)

ABSTRACT

Hydrocarbon injection experiments have been performed to investigate the chemical sputtering yield of CFC at elevated temperatures (T*surface* ≅ 500K) and detached plasma conditions in the JET outer divertor. A plasma scenario in L-mode with the outer strike-point on the load bearing septum replacement plate was developed to detach the divertor and to provide the recombining target plasma. The operational window was explored in a set of discharges with strong deuterium puffing into the private flux region. Langmuir probes showed a clear roll-over in the ion flux up to complete detachment at the target during the density ramp. Paschen recombination line analysis shows strong volume recombination with $T_e < 2{:}0eV$ prior to the appearance of an X – point Marfe. A strong reduction of the intrinsic *CD* photon flux was observed under these conditions in which local CD_4 injection clearly led to *CD* photon flux emission. This provides conclusive evidence for a reduction of the hydrocarbon flux and the chemical sputtering.

1. INTRODUCTION

Detached divertor operation is mandatory on ITER to reduce the expected high heat loads on Plasma-Facing Components (PFCs) - in particular on the divertor target plates made of Carbon-Fibre Components (CFC) and/or tungsten - to manageable levels [1]. Divertor detachment is caused by low electron temperature/recombining plasma operation at high electron densities. The impact energy of fuel ions drops below the threshold for physical sputtering so that for CFC targets, only chemical sputtering remains as a source for the impurity in flux close to the strike-point areas [2].

Chemical sputtering can be described as a function of ion energy, ion flux and surface temperature [3], though uncertainties with respect to data interpretation and extrapolation to detached plasma conditions exist. Recent experiments in Asdex-Upgrade and DIII-D at low surface temperatures ($T_{surface} \simeq 350$K) showed a reduction of the intrinsic hydrocarbon flux and the chemical sputtering yield under detached conditions in comparison to attached conditions in high density plasmas [4,5]. A reduced carbon source is favourable for the minimisation of carbon migration and the subsequent appearance of co-deposited fuel in carbon layers. Carbon which is necessary to radiate in the divertor to obtain/maintain the divertor detachment is eroded in the scrape-off layer SOL spatially away from the strike-zone on the target plane [2]. Seeding impurities such as argon will be applied in addition to increase the radiative fraction. Chemical sputtering at these low $T_{surface}$ is caused by ion induced desorption of hydrocarbon radicals and not by thermal emission of hydrocarbon radicals enhanced by radiation damage as described in [3]. The later mechanism will dominate the chemical sputtering in ITER at the expected target temperatures.

An experiment at JET with detached outer divertor leg has been performed to investigate the sputtering yield at $T_{surface} \simeq 500$K, closer to the maximum temperature of chemical sputtering. Quantifcation of the chemical sputtering is done in-situ with spectroscopy on the hydrocarbon break-up product CD in combination with local CD_4 injection [4] into the near outboard SOL through a single injection module. This experiment focuses on both the exploitation of steady-state detached

divertor operation with carbon PFCs and the determi- nation of the carbon erosion under these conditions.

2. EXPERIMENTAL SET-UP AND PLASMA SCENARIO

A plasma scenario in lower single-null configuration with the outer strike-point OSP fixed on the centre of the load bearing septum replacement plate LBSRP was developed to detach the outer divertor leg (at the local injection location) with the aid of strong deuterium fuelling. The experiment was performed in L-mode with moderate additional heating (P_{aux} = 1:8MW NBI) and at high magnetic field (Bt = 2:7T, Ip = 1:8MA) to ensure operation below the L – H transition threshold. A magnetic configuration with medium triangularity (δ = 0:39) and large distance between the separatrix and the top of the machine (30cm) is chosen to reduce the plasma-wall interaction in the main chamber. The poloidal length of the inner di- vertor leg with a maximum distance of 8:5cm between the X – point and the inner strike-point was short in comparison with the outer leg with 13cm distance between X – point and tile 5 (LBSRP) (figure 1a). This short poloidal distance actually reduces the ease with which the inner divertor detaches, in contrast to more balanced divertor geometries at JET, where the inner target is often completely detached, even for moderate densities in L – mode plasmas.The configuration was optimised for both access to {transient and feedback-controlled{ de- tached divertor plasma operation and the in-situ calibration of the eroded hydrocarbon flux using spectroscopy and local gas injection. The operational window for feedback-controlled outer divertor detachment was explored in a set of discharges with strong deuterium puffng into the private-flux region. Deuterium was injected through a circumferential gas injectionmodule located in the base plate of the inner divertor (labelled GIM11) and ramped-up (with maximum fuelling rates up to 1:4 $\times 10^{22}$D/s) to the density limit. The transition from an attached to a detached divertor plasma was determined by the roll-over of the ion flux, Γ_D+ measured with the aid of a set of Langmuir Probes (LP) embedded in the LBSRP and the appearance of deuterium volume recombination monitored spectroscopically. The increase of the central density and the neutral pressure in the subdivertor with the D_2 injection ramp as well as the power balance between total input and radiated power is shown in figure 1b for the representative discharge #70574. Several reproducible pulses were performed to vary diagnostic settings for best characterisation of this transient regime. The discharge terminates rapidly in a density limit disruption for radiated powers beyond 80%. Steady-state detached divertor operation with a °at-top phase of about 6s was achieved by real-time feedback control on the edge density with the injection rate as actuator. Time traces of global parameters are depicted for the representative discharge #70584 in figure 1b, too. Oscillation between detached and attached divertor operation occurred if the gain factor was set to high (#70580). This oscillation was used to compare attached and detached plasma operation in a single discharge.

A number of diagnostics are used to characterise the cold and dense divertor plasma. The tile embedded LP (KY4D [6]) and Paschen/Balmer recombination spectroscopy (KT3) provide T_e and n_e, radiated powers are obtained with the divertor bolometry system (KB5 [7]) and the divertor neutral

density n_D is supplied by a sub-divertor neutral pressure gauge (KT5P). In-situ the hydrocarbon flux Γ^{CD} and the incident particle fluxΓ^{D} are obtained with the aid of divertor spectroscopy (KS3 [4]) and local CD_4 injection (GIM14). Figure 1a illustrates the detection coverage of the toroidally separated diagnostics in one toroidal plane of the divertor.

3. CHARACTERISATION OF THE DETACHED OUTER DIVERTOR PLASMA

The degree of detachment DOD [8] provides a normalisation criterion for the increase of the ion flux with upstream plasma density, at constant power flux into the edge plasma, compared with the expected dependence high recycling case ($\Gamma D+ \sim n_e^2$). Figure 2 shows the time evolution of both DOD, related either to the separatrix or integral ion °uxes onto the LBSRP during the density ramp of pulse #70574 normalised to the start of the high recyclingphase at 19.2s. The LP at the OSP showed a clear ΓD+ roll-over during the density ramp at t = 20.7s, indicating the beginning of the detachment process and a linear increase of both DOD^{sep} and DOD^{int}. The faster rise of DOD^{sep} indicates that the detachment starts at the separatrix and extends to the SOL. At t = 22:5s the SOL at the LBSRP is almost completely detached, and Marfe formation at the X-point gradually sets in. The corresponding changeof the peaked profile at the target ($T_e = 50eV$ and $n_e = 1.2 \cdot 10^{19} m^{-3}$) to an almost flat profile with significantly reduced values down to $T_e < 10$eV and $n_e < 4 \cdot 10^{19} m^{-3}$ is depicted in figure 3a.

Detachment is mandatory but not sufficient for the appearance of volume recombination in the divertor. Significant volume recombination sets in at T_e below ≃ 5eV [9]. Here, volume recombination was detected in the outer leg using analysis of the Paschen and/or Balmer recombination lines [9]. The Stark broadening of high-n lines (n = 7 - 9) provides the n_e distribution at the LBSRP shown in figure 3b. Using both the Paschen continuum and the line ratios of the n = 10 – 12 lines, Te < 2.0eV is found at the OSP (figure 3b) at t = 22:5s. The time evolution of the $Paschen^{-2}$ line (figure 3b) shows that the volume recombination begins at the OSP and extends into the SOL as time and density increase, confirming that partial detachment in this magnetic configuration occurs first near the OSP. This spectroscopic observation of intense deuterium volume recombination is an irrefutable indicator of a low T_e plasma in the outer divertor and is entirely consistent with the strong reduction in the local ΓD+ to the plate. And yet, although the LP temperature profile (figure 3a) collapses across tile 5, it is never much lower than $T_e \cong 10eV$. This situation is extremely reminiscent of observations reported on TCV [10] where the standard divertor geometry, with a long outer and much shorter inner divertor leg, is similar to the JET configuration used here. Despite the strong outer target detachment seen in low power, density ramp experiments, the plate T_e, measured by tile embedded LPs, never fell to the low values expected in a detached plasma. The latter is also characterised by strong parallel temperature gradients in the X – point vicinity, followed by an extended convective region of low T_e down to the target. The high measured T_e is therefore very likely due to a small population of electrons from further upstream, travelling collisionlessly to the target LPs.The total radiation reconstructions shown in figure 3c are also consistent with a picture

in which the rather open nature of the chosen divertor configuration allows carbon impurities and deuterium neutrals to readily escape the outer target region. Radiation then occurs preferentially in the higher T_e plasma in the X – point vicinity, leading to enhanced power exhaustion (and stronger detachment) as heat fluxes arriving from the main SOL encounter the strongly radiating region.

4. IMPACT OF DIVERTOR DETACHMENT ON THE HYDROCARBON FLUX

A direct comparison between attached and detached divertor operation is made in a single shot to study the impact of detachment on the carbon impurity source distribution and strength. Both the reduced impact energy and the increase in the total incident particle flux induced by detachment have an impact on the chemical sputtering. Figure 4a shows the spatial distribution at the outer target of the CD Gerö band, indicator of the hydrocarbon flux, and the CII line (426.7nm), indicator of the total carbon flux. The corresponding integrated photon fluxes $\phi^{intrinsic}_{CD}$ and $\phi^{intrinsic}_{CII}$ are given in figure 4b together with the D_γ photon flux $\phi_{D\gamma}$. The D_γ light pattern shows a strong increase starting at the OSP close to the roll over of Γ_D+ and extending to the SOL. This is in contrast with the light pattern of both carbon transitions which show a strong reduction coincident with the D_γ increase. Surprisingly the maximum emission of the CD Gerö band in the high recycling regime is separated a few cm spatially away from the OSP into the SOL. The maximum emission of the CII line is, however, well correlated with the location of the OSP in both the attached and the high recycling phases, suggesting that in addition to chemical sputtering, physical sputtering also contributes to C^+. The strong reduction of $\phi^{intrinsic}_{CD}$ by about a factor 5 between t = 19:5s and t = 22:5s can be divided into two phases in which the first (steep slope) one occurs in the high recycling phase and the second (flat slope) in the detached phase. The CD light pattern is consistent with this division: the first reduction occurs all over the target in the SOL whereas during the second, the remaining CD is located close to the ionisation front. This CD light source diminishes as the DOD increases. The $\phi^{intrinsic}_{CD}$ shows a slow and less pronounced reduction to half the initial value in the detached phase with a slope similar to that found for the the second phase of $\phi^{intrinsic}_{CII}$ decay.

To calibrate the hydrocarbon flux, CD_4 was injected through GIM14 located toroidally between two modules of tile 5 into discharges with density feedback control. Figure 5a) shows the injection into a shot with oscillation between divertor attachment and detachment. The extrinsic photon flux $\phi^{intrinsic}_{CD}$ could clearly be detected with the integral line-of-sight of KS3 of 20cm diameter centred on the injection valve to ensure as large coverage of the emission cloud (figure 1a); a loss of photons out of the observation volume under detached conditions cannot be fully excluded. Since only pulsed injection was possible and the pulse length extends for times longer than the attached-detached oscillation frequency, the pulse shape is accounted in the analysis. The extrinsic CD A-X photons in both phases are detectable (figure 5a), but photon e±ciencies in the recombining (detached) and ionising (attached) plasma differ by 35%. The absolute quantification of the effective inverse photon efficiency $\left[\frac{D}{XB}\right]^{CD_4 \longrightarrow CD}_{A^2\,\Delta \longrightarrow X\ ^2\Pi} = 45 \pm 22$ in the detached phase was performed in discharge # 70582 with constant density (figure 5b). The slight change of $\left[\frac{D}{XB}\right]^{CD_4 \longrightarrow CD}_{A^2\,\Delta \longrightarrow X\ ^2\Pi}$ in attached and detached

plasmas cannot account for the strong reduction of $\phi^{intrinsic}_{CD}$ by a factor 4.8. This suppression of $\phi^{intrinsic}_{CD}$ is then caused indeed by the reduction of $\phi^{intrinsic}_{CD_4}$ by more than a factor 3.1 in the detached plasma in comparison to the attached plasma, thus, by the reduction of the chemical erosion source.

SUMMARY AND CONCLUSION

The experimental observations can be summarised as followed:

- Outer divertor detachment with recombining plasma established.
- CD_4 injection leads to significant extrinsic CD A–X photon °ux.
- Strong reduction of the hydrocarbon flux as soon as D_γ starts to rise.
- Almost complete suppression of chemical erosion with detached outer leg on the LBSRP and recombining plasma with $T_e < 2{:}0eV$.

This experiment confirms the reduction of the chemical erosion yield under detached and recombining plasma conditions close to the maximum surface temperature of erosion.

REFERENCES

[1]. G. Federici *et al*., Nucl. Fusion **41** 12R (2001) 1967
[2]. A. Kirschner *et al*., J. Nucl. Mater. **363-365** (2007) 91
[3]. J. Roth *et al*., Nucl. Fusion **44** L21 (2004)
[4]. S. Brezinsek *et al*., J. Nucl. Mater. **363-365** (2007) 1119
[5]. S. Brezinsek *et al*., Physica Scripta **T128** (2007) 40
[6]. S. Jachmich *et al*., J. Nucl. Mater. **363-365** (2007) 1050
[7]. A. Huber *et al*., J. Nucl. Mater. **363-365** (2007) 365
[8]. A. Loarte *et al*., Nucl. Fusion **38** 3 (1998) 331
[9]. ADAS http://adas.phys.strath.ac.uk
[10]. R.A. Pitts *et al*., J. Nucl. Mater. **290-293** (2001) 940

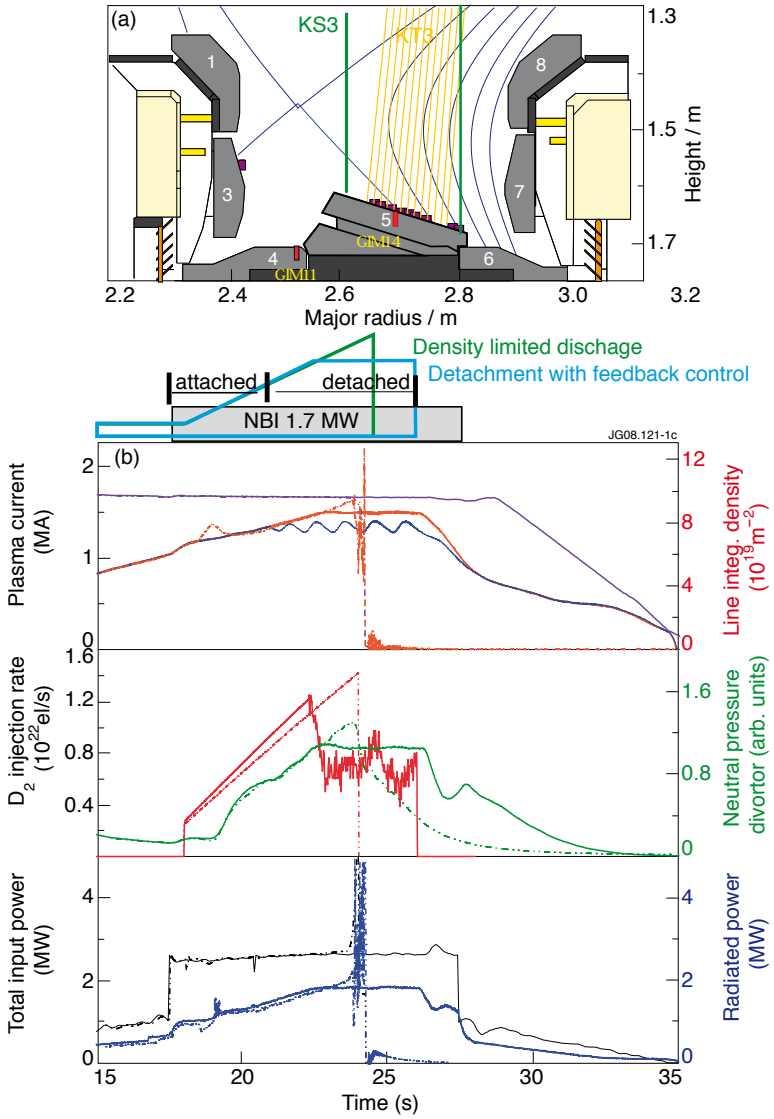

Figure 1: a) Magnetic configuration and diagnostic coverage in the divertor. b) Time traces of global parameters for transient and steady-state detached divertor operation.

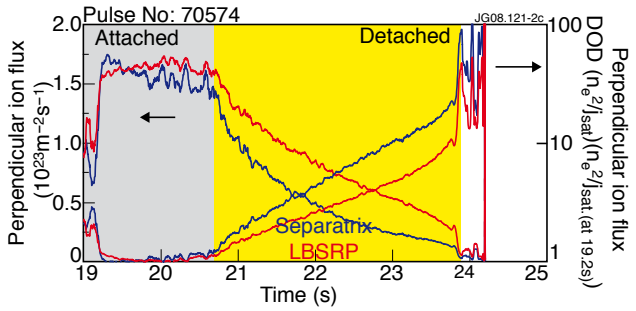

Figure 2: DOD and Γ_{Dk} in the outer divertor during the density ramp-up.

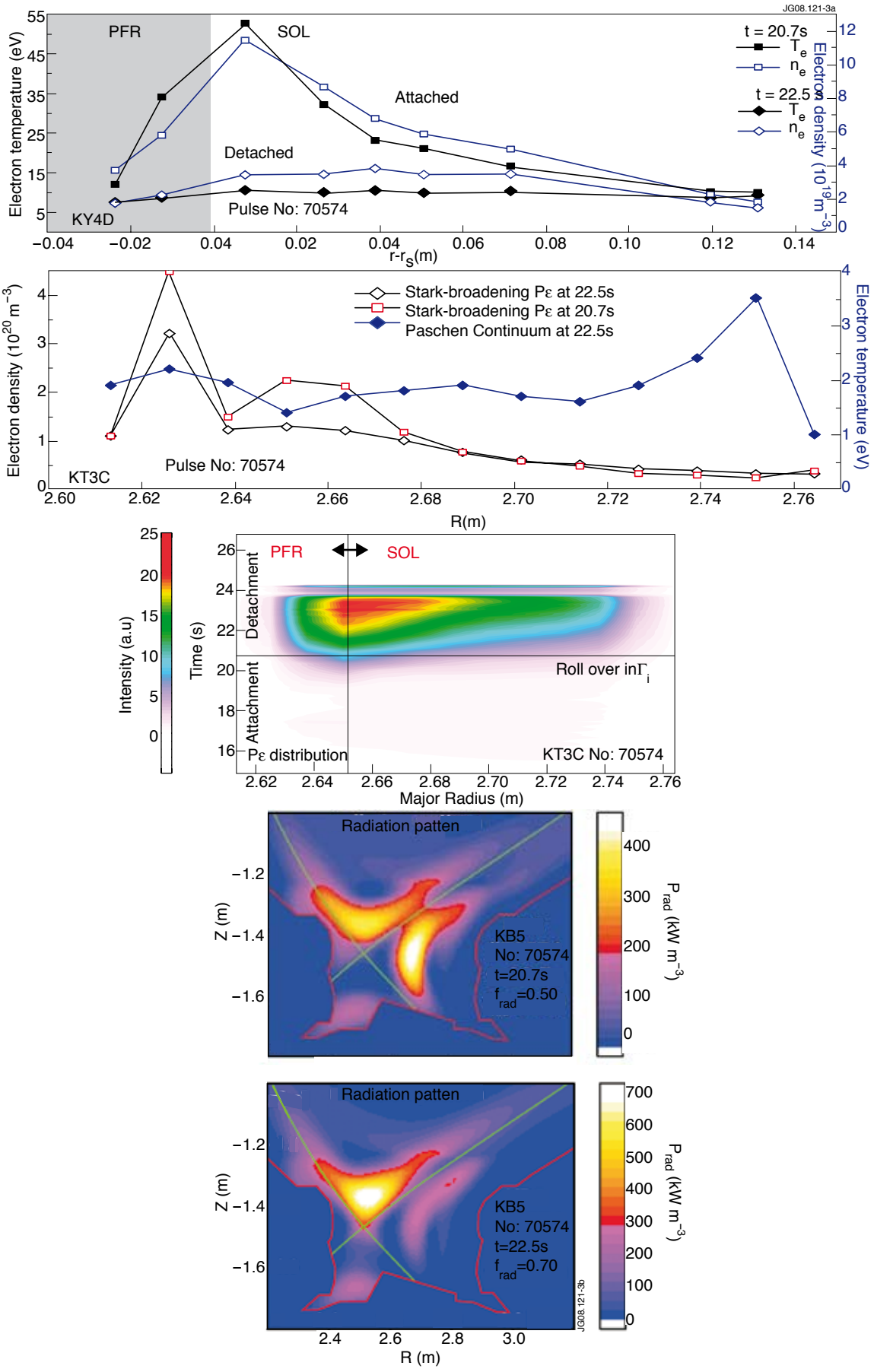

Figure 3: Plasma characterisation in the outer divertor leg during high recycling (t = 20:7s) and detachment (t = 22:5s). a) T_e and n_e profiles deduced from LP, b) T_e and n_e profiles deduced from Paschen recombination, c) radiation pattern.

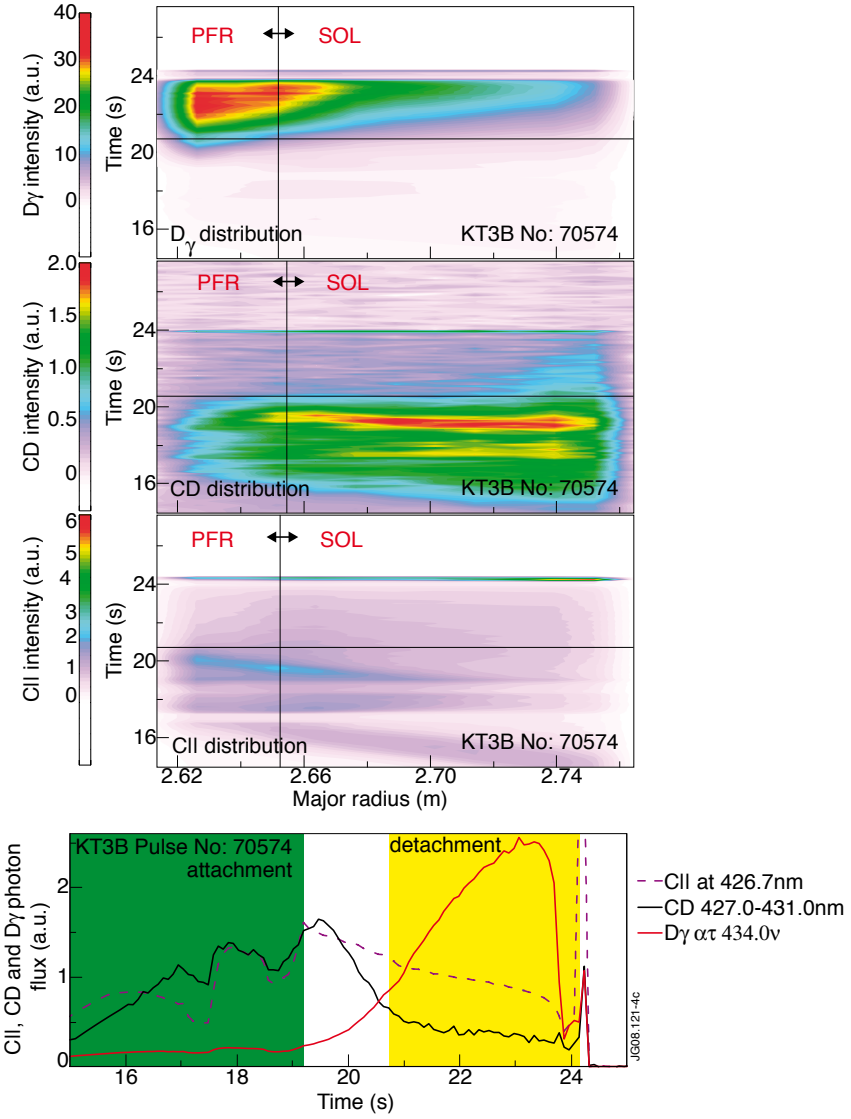

Figure 4: a)Spatial distribution of D_{γ}, CD A-X band, and CII in the outer divertor during the transition from attached to detached plasma operation. b) Time evolution of the integrated photon fluxes.

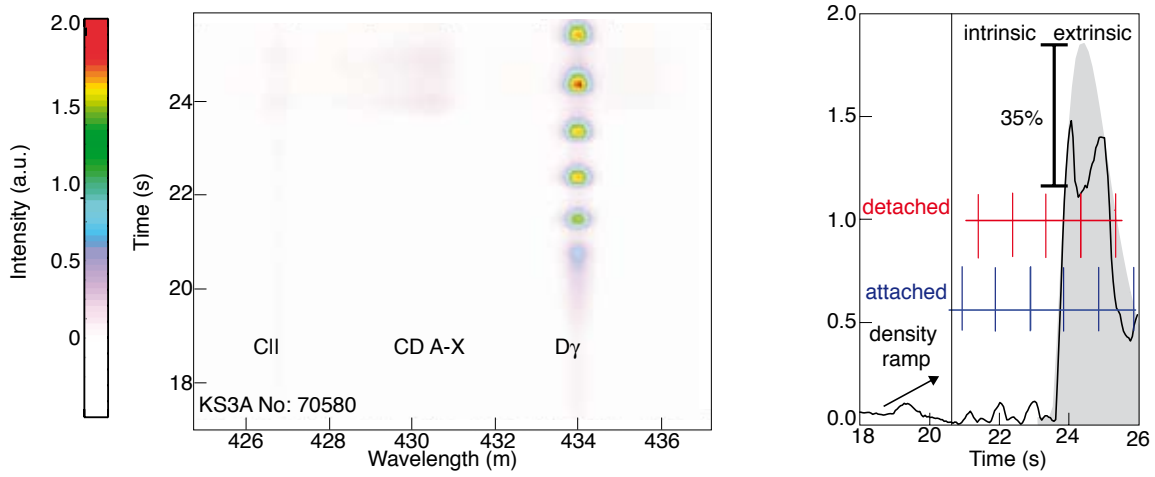

Figure 5: CD A-X band emission under attached and detached plasma conditions with local CD_4 injection.